https://doi.org/10.48048/tis.2023.5664

Spatio-Temporal Variations of Climate Variables and Extreme Indices over the Aral Sea Basin during 1960 - 2017

Berdimbetov Timur

Nukus branch of Tashkent University of Information Technologies named after Muhammad-al Khorezmi, Tashkent, Uzbekistan

(Corresponding author's e-mail: timur.berdimbetov@tea.ac.cn)

Received: 19 August 2022, Revised: 27 November 2022, Accepted: 4 December 2022, Published: 10 September 2023

Abstract

The Aral Sea plays a key role in the socio-economic development of Central Asia. In the past few decades, with the combined effects of global warming and human activities, the ecological environment of the Aral Sea has undergone significant changes, such as the reduction of the basin area and the drop in water levels. In this study uses the observed climate data, combined with remote sensing to systematically analyze the characteristics of changes in climate in the Aral Sea Basin (ASB). We used linear regression, Pearson's correlation and Pettit's test to determine climate change. The main conclusions are as follows. Based on the analysis of the temporal and spatial changes of temperature, precipitation, and potential evapotranspiration in the Aral Sea Basin from 1960 to 2017, it was found that the annual average temperature, precipitation, and potential evapotranspiration increased by 0.32 °C decade^{-1}, 0.16 mm decade^{-1}, and 0.04 mm day^{-1} decade^{-1}, respectively. In addition, the changes of these climatic variables were different in the growing season (April - September) and the non-growing season (October - March). Temperature and potential evapotranspiration increased in both growing and non-growing seasons; however, the precipitation decreased (increased) in the growing (non-growing) season. This means that the climate in the growing season showed a warming and drying trend.

Keywords: Climate change, Temperature, Precipitation, Potential evapotranspiration, Climate extreme indices, Aral Sea

Introduction

Central Asia is the largest semi-arid region in the world and one of the regions that have been affected the most by climate variability [1-3]. The temperature change is higher than the global mean [4,5] the precipitation indicates an increase in very small quantities. However, regional trends at the level of areas and valleys can differ significantly from these observations due to the complexity of the topography and different atmospheric conditions. Biophysical consequences of changing climatic regimes are likely to include melting glaciers, changing seasonality of river flow regimes causing seasonal water shortages or changing vegetation patterns [6,7]. This is so because given that the natural resources are already limited, livestock and agriculture can negatively affect the permanent lifestyle in mountainous areas [7]. Therefore, it is important to analyse the spatial and in situ changes in temperature and precipitation over time. Moreover, such studies, in turn, play an important role in providing inputs for adapting agriculture and people's lifestyles to the phenomenon of climate change in the Central Asia region as per the requirements in the different geographical locations therein.

Past studies have focused primarily on the analysis of climate variability in specific sub-regions, such as the Himalayas [8], Tien Shan [9], the Pamirs [10] and other regions where climate variability has been studied separately [1]. One of the main reasons for the separate organisation of these areas has to do with the problem of the water resources in this region as the mountains located in these regions are the origins of the region's rivers and the key sources of these regions' water. Other studies have focused on the temperature [11] or precipitation [12] trends in the topographic complexity, covering the entire territory of Central Asia. All these studies have noted a strong trend in temperature, especially in recent decade [11,13]. Temperatures are especially high in the Tien Shan and the Himalayas, and precipitation falls in the northwest, where western

regions prevail. While there is a general trend towards increased precipitation, regional differences between lower and higher altitudes are evident [13].

Studies on climate variability in the Central Asia region reveal varied results. One of the main reasons for this is the different datasets used by them. In past studies, climate analysis using gridded products was based on the data received from meteorological stations [12,14,15] or local meteorological stations established since the early 20th century [4,16]. The results can therefore differ because the accuracy and integrity of the data varied in the location densities of these meteorological stations and the low-altitude and proximity of the location points. Therefore, in the analysis of climate change in Central Asia, the following gridded climate databases, based mainly on global climate databases, were used in the earlier studies: CRU [17], the GPCC [18], or NASA's Tropical Rainfall Measuring Mission (TRMM) [19], etc.

In this paper, we present the complex and detailed analysis that we performed by combining temporal and spatial changes in key climate parameters (temperature (TMP), precipitation (PRE) and potential evapotranspiration (PET) in the entire ASB and its sub-regions (Low part of ASB, Mid part of ASB and Upper part of ASB). So far, such a combined approach has been adopted only by a few studies [15,20-25], and these studies are not focused on the ASB. Seasonal changes in temperature and precipitation patterns are the key parameters that provide the general overview of past climatic changes as far as this study region (i.e. Central Asia) is concerned because under the effects of climate variation, there are still large uncertainties in the response of climate extremes [26]. In this study, we have tried to understand the spatiotemporal trends of climate parameters over the ASB.

Materials and methods

Datasets

In this study, we shall discuss the climate factors we referred to such as TMP (monthly), PRE (monthly) and PET (daily) from the CRU TS 4.02 dataset, University of East Anglia (https://crudata.uea.ac.uk/cru/data). The CRU dataset covers all land areas (except Antarctica) and for the period from 1901 to 2017 (at a spatial resolution of 0.5×0.5 degrees), and it is constructed based on monthly observational data from land meteorological stations across the world.

The CRU dataset is based on a large number of stations with good quality control and homogeneity check [27]. Before using the CRU dataset, we evaluated the performance of the CRU data over the study region (**Figure 1**). For this purpose, we selected meteorological stations from the upper (Khatlon station), middle (Karshi station) and lower (Chimbay station) parts of the basin, and we compared their data with the corresponding grid cell of the CRU dataset where the station is located. From 1960 to 2015, the observed rainfall and temperature measured in the stations located at the upper and lower parts of the basin showed high correlation with the CRU datasets (**Figures 1**(**a**) and **1**(**c**)). A comparison of station-based observations with the CRU data indicated that the mean annual precipitation in both datasets is closely associated. For instance, there is a high correlation between observed rainfall and calculated rainfall from CRU in all the selected stations with the coefficient values 0.93, 0.80 and 0.94, respectively (**Figures 1**(**d**) - **1**(**f**)). Similarly, concerning temperature also a strong correlation was found among the 2 data sources.

Our comparison is fully consistent with previous research. In order to evaluate performance of CRU, Haag *et al*. [1] calculated the correlation coefficient between CRU and data of 14 stations located on the territory of Central Asia (for temperature in 1950 - 2016, and precipitation in 1998 - 2016). They found that CRU shows a high correlation with registered temperature and precipitation, and confirmed that station data is very likely included in the original CRU dataset [28]. Similarly, Chen *et al*. [29] used CRU temperature and precipitation data to analyze glacier/snow cover change in the Central Asian part of the Tienshan Mountains in 1960 - 2014 years. Guo *et al.* [30] also analyzed the drought process change in Central Asia from 1966 to 2015 based on monthly precipitation and potential evaporation data from the version CRU TS4.00.

As such, the climate index was used to calculate daily climate index data from the World Meteorological Organization database [31,32].

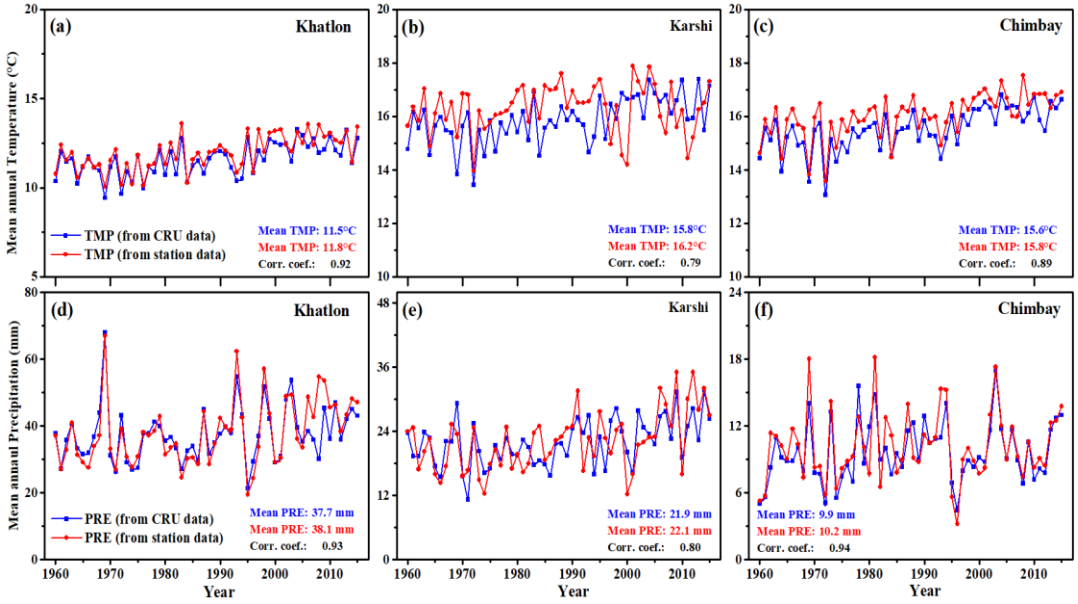

Figure 1 Compare CRU and station data: (a) - (c) mean annual Temperature (TMP, ℃) and (d) - (f) mean annual Precipitation (PRE, mm). The blue line is CRU data, and the red line is station data.

Methodology

In this paper, the various methods that were used in this study to analyse climate change have been discussed. Initially, for spatial analysis, the part of the CRU data belonging to the study area was extracted using an ArcGIS 10.1 extract by mask, and interpolation was performed on each grid cell using the spline interpolation method to interpolate average climate variables for each grid cell in the total area. This interpolation method has been successfully used in past studies to analyse climate change in Central Asia [33, 34]. In analysing the spatial trend, we used a special "trend" package from RStudio. In analysing the time series concerning climate change in this region, we used the linear regression method, which is good for a time series whose data are increasing or decreasing at a constant rate.

A mathematical equation that evaluates linear regression is:

$$y = a + bx + \varepsilon \quad (1)$$

x is the independent variable or predictor, and y represents the dependent or response variable. This is the value we expect for y (on average) if we know the value of x, i.e. this is the "predicted y-value." a is a free term (intersection) of the line of assessment; b is the slope ratio or gradient of the estimated line; it represents the amount by which y increases on average if we increase x by one. ε is the residual error. In addition, based on Pettitt's non-parametric method, we determined the change point in climate factors.

The software packages for data homogenization (RHtestsV4) and index calculation (RClimDex) are based on the very powerful and freely available R statistics package that runs with both Microsoft Windows. The Climate index was calculated using the RClimdex program, a special package of RStudio [35].

Change Point Detection: Pettitt's test for change detection, developed by Pettitt, is a non-parametric test that is useful for evaluating abrupt changes in climatic records [36]. The Pettitt test is the most commonly used test for detecting a change point due to its sensitivity to breaks in the middle of any time series [37].

Results and discussion

Spatial distribution of climate parameters in the ASB

Over the past few decades, global warming and regional desiccation have been acute problems due to their major global effects. These processes are also serious in the Central Asia region. As shown in **Figure 2**(**a**), in climatology, the mean annual TMP rises from the northern part to the southern part of the ASB. The highest

temperature in the southeast of the basin is 18 - 20 ℃. In mountainous areas, the mean annual temperature is around 0 ℃. In the ASB, the mean annual temperature is 11 ℃. The high temperature (15 - 20 ℃) distribution scale covers 28.31 % of the area; the relatively low-temperature distribution (11 - 13 ℃) covers 26.49 %, and the very low temperature (0 ℃) distribution covers 9.83 % of the full area.

The spatial distribution of mean annual precipitation (**Figure 2**(**b**)) decreases from the upper part of the basin to the southwest with the lowest value (11 - 15 mm) prevalent in the desert areas around the Aral Sea, north of Turkmenistan and northeast of Uzbekistan. The distribution of high precipitation (55 - 65 mm) is in the mountainous zones of Tajikistan, Kyrgyzstan and Uzbekistan. The distribution of very low (11 - 15 mm) and low (20 - 30 mm) precipitation values account for 44.23 and 28 %, respectively. The moderate (35 - 45 mm) and high precipitation distribution (55 - 65 mm) account for 18.74 and 9.03 %, respectively. The distribution of PET resembles the distribution of temperature, i.e. high PET in areas where high temperatures are observed and vice versa (**Figure 2**(**c**)). PET value was 44.31 %, with a high PET (3.8 - 4.2 mm day^{-1}) occupying a large area and a low PET (2.2 - 2.6 mm day^{-1}) distribution observed in the region of 15.61 %.

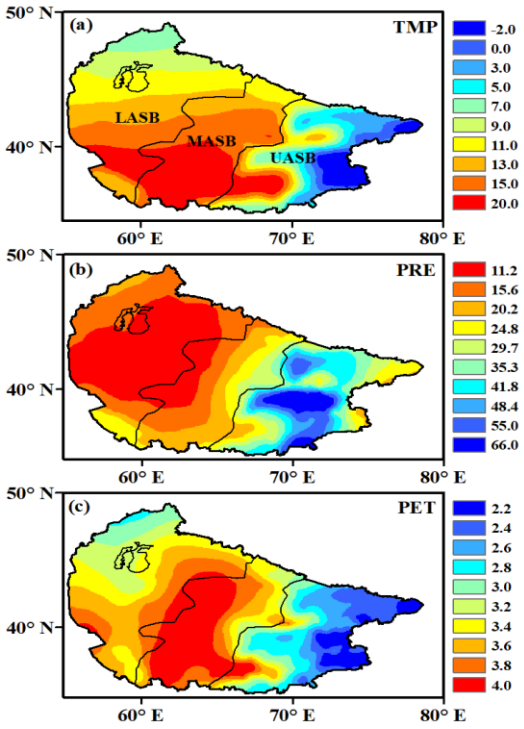

Figure 2 Spatial distribution of long-term climatology (1960 - 2017 year) of (a) Temperature (TMP, ℃), (b) Mean annual precipitation (PRE, mm) and (c) Potential Evapotranspiration (PET, mm day^{-1}). Thick and thin black lines show the borders of ASB and the Aral Sea, respectively. UASB, MASB and LASB denote the upper, middle and lower parts of the basin (black boundary), respectively.

Spatial distribution of trend of climate parameters in the ASB

Figure 3 shows the spatial distribution of linear trends of climate parameters. Between 1960 and 2017, the mean annual temperature showed significant positive trends in all parts of the ASB (**Figure 3**(**a**)), with an average trend value of 1.23 ℃ decade^{-1}. Higher trends (1.7 - 1.9 ℃ decade^{-1}) were observed for the central and southwestern part of the ASB, including for the Aral Sea itself, accounting for 45.79 % of the area. Significant low trends for the changes (0.9 - 1.1 ℃ decade^{-1}) were observed in a small area in the southeastern part of the ASB, which accounted for 9.96 % of the total area. Significant moderate trends (1.3 - 1.5 ℃ decade^{-1}) occupied 44.25 % of the ASB, with its spatial distribution flowing towards the centre of the basin.

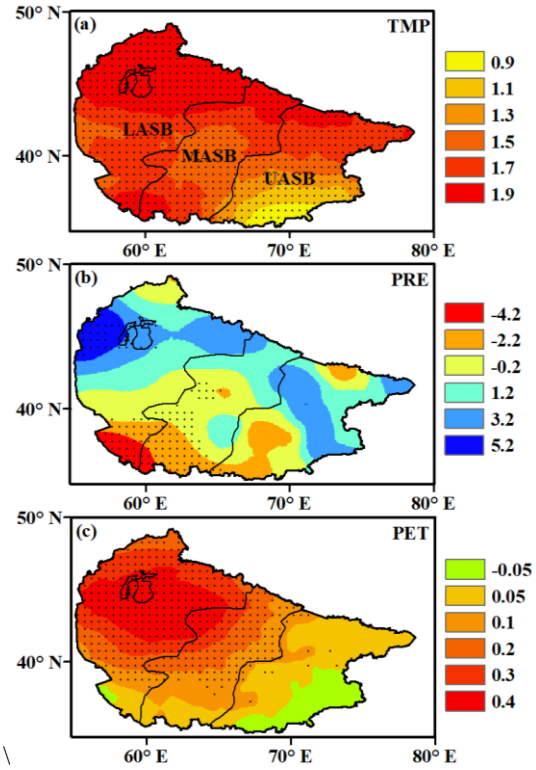

Figure 2 Spatial distribution of linear trends of climate variables in the ASB from 1960 to 2017. (a) Temperature (TMP, ℃ decade^{-1}), (b) Annual precipitation (PRE, mm decade^{-1}), (c) Potential evapotranspiration (PET, mm day^{-1} decade^{-1}). Thick black line is border of the ASB, thin black line is Aral Sea border. Significant trends are indicated by dots. The UASB, MASB, LASB denote upper, middle, and lower of the basin, respectively.

For the distribution of the trends of annual precipitation (**Figure 3**(**b**)), low negative (-0.2 mm decade^{-1}) trends were recorded in a large part of the basin, including around and near the Aral Sea and in the centre of the basin. In the southwest of the basin, incredibly low (-4.2 mm decade^{-1}) trends were observed in a small area. Further, significant low positive trends were found over the Aral Sea. Significant high positive trends (3.2 - 5.2 mm decade^{-1}) prevailed over the initial part of the basin and mountainous areas. Precipitation decreased in 57 % of the basin, while it increased in the remaining 43 %. For the PET (**Figure 3**(**c**)), increasing trends were found significantly in all parts except the small area in the southeastern part of the basin. Positive spatial trends of PET were distributed over 90.7 % of the region. High significant positive trends (1.9 mm day^{-1} decade^{-1}) were observed over the Aral Sea.

Temporal change of climate variables in the ASB

In this section, we analyzed the time series of climate variables. Firstly, based on Pettit's test [38], we employed a non-parametric method to determine the change point in TMP, PRE and PET. For all 3 variables, this method identified the changing point around the year of 2000 (**Figure 4**). Therefore, 2 corresponding time intervals (1960 - 2000 and 2000 - 2017) were chosen for further analysis of climate change in addition to the full study period (1960 - 2017).

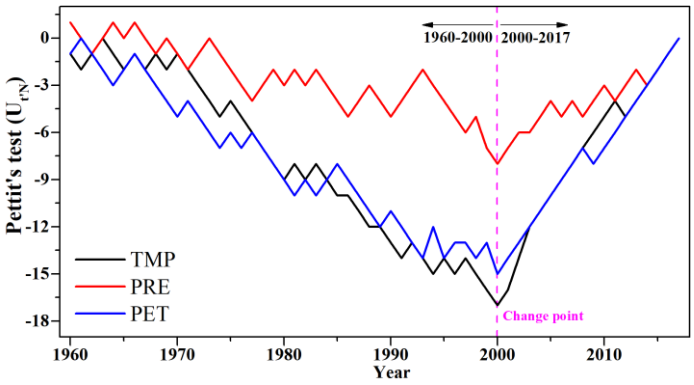

Figure 3 Abrupt change point detection of Temperature (TMP; black line), Precipitation (PRE; red line), and Potential evapotranspiration (PET; blue line) using the Pettit test for the period 1960 - 2017 over ASB.

Our hypothesis is fully consistent with the past studies demonstrating that the climate in Central Asia was developing differently before and after the year 2000. In particular, Guo *et al*. [30], in their analysis of changes in the drought situation in Central Asia from 1960 to 2015, assumed 2000 as a change point in temperature and precipitation. Jiang *et al*. [39] also analysed the LD change in the lower part of the Amu Darya River for the period 1990 to 2017 and determined that 2000 is a mutation year on the basis of the changes in temperature and precipitation.

According to the results of the analysis, during the full study period (**Figure 5**(**a**)), the annual TMP increased significantly (0.32 ℃ decade^{-1}, 90 % confidence level). The annual TMP trend was positive (0.26 ℃ decade^{-1}) during the 1st period (1960 - 2000). From 2000 to 2017, the mean TMP value was 9.4 ℃, and this period is hotter compared to the period from 1960 - 2000. Although a negative trend (-0.05 ℃ decade^{-1}) was recorded during this period, it was caused by high temperatures in 2000, 2003 and 2004 with mean values of 9.8 - 9.9 ℃ and cold years 2012 and 2014 with temperatures of 8.5 and 9.1 ℃, respectively.

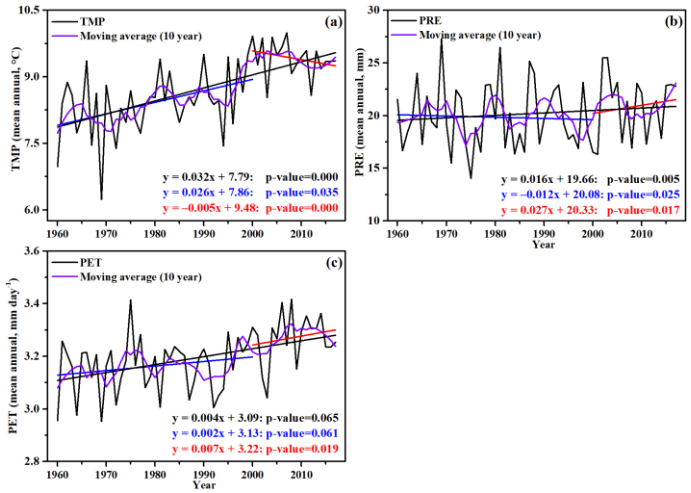

Figure 4 Temporal change of climate variables (a) Temperature (TMP, °C), (b) Precipitation (PRE, mm) and (c) Potential evapotranspiration (PET, mm day^{-1}) from 1960 to 2017. The black, red, and blue straight lines represent the linear trends for the periods 1960 - 2017, 1960 - 2000 and 2000 - 2017, respectively.

During the full study period, PRE (**Figure 5**(**b**)) shows a weak positive trend (0.16 mm decade^{-1}), while the PRE trend value decreased in the 1st period (-0.12 mm decade^{-1}) and increased in the 2nd (0.27 mm decade^{-1}). PET shows positive trends in all the periods with a high trend value observed during 2000 - 2017 (0.07 mm day^{-1} decade^{-1}).

Analysis of climate extreme indices in the ASB

According to numerous studies [40-42], under conditions of intensification of global warming, the frequency of many extreme weather and climate events increases. Analyzing extreme climate changes is very important in regions where the economy is dependent on agriculture because with the help of the extreme climate index, we can determine the time of season change in the regions. In this regard, the World Meteorological Organization (WMO) and the International Panel of Experts on Climate Change (ETCCDI) have developed 27 main indices characterizing extreme climate index and recommended that individual countries conduct studies of these indices to generalise and use them to assess climate change in large regions or for the globe as a whole [35]. These indices include climatic extremes, the number of cold, frosty and hot days, tropical nights and indices based on, among others, distribution percentiles and the number of rainy and dry periods. Using data from the Daily Meteorological Station, we analysed changes in the climate extreme index in the ASB region based on temperature and precipitation changes as detailed below [43]:

1) Frost Days (FD): The number of frost days during the year, t is taken as a daily minimum temperature (T_{min}) less than 0 ($T_{min} < 0$ °C).

2) Summer Days (SD): The number of warm days during the year, t is taken as a daily maximum temperature (T_{max}) greater than 25 °C ($T_{max} \geq 25$ °C).

3) Growing Season Length (GSL): t – if we take it as a daily mean temperature (T_{mean}), the number of mean daily temperature greater than 5 °C ($T_{mean} \geq 5$ °C).

4) Consecutive Dry Days (CDD): The maximum number of dry days with less than 1 mm precipitation.

The territory of the ASB is geographically composed mainly of plains, while the upper part of the basin is mountainous. The climate is uneven throughout the year with mostly continental and severe drought days in the plains and more wet days in the mountains. To analyse the above climate index changes, 6 meteorological stations in the ASB area were selected: Naryn and Khatlon from the UASB, Tashkent and Karshi from the MASB and Chimbay and Kazalinsk from the LASB. Climate extreme changes were analysed based on the available daily data obtained from these meteorological stations and using the RStudio program.

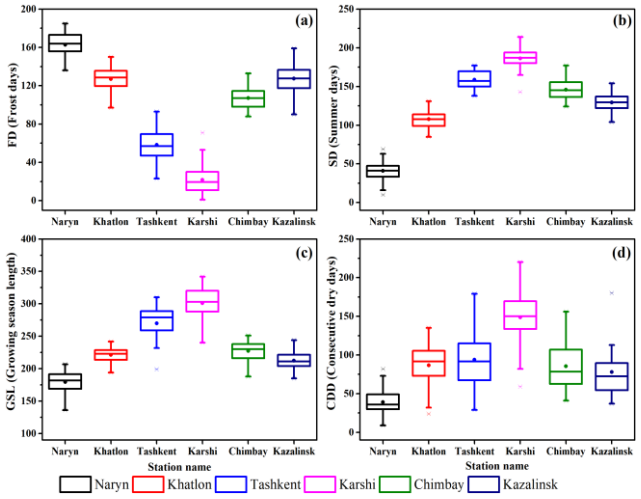

Figure 5 Box plot of extreme of climate index change in the territory of ASB. (a) Frost days (FD, day), (b) Summer days (SD, day), (c) Growing season length (GSL, day) and (d) Consecutive dry days (CDD, day). The long-term mean of each climate index value in different stations is indicated by a dot, while 99th and 1st percentile climate index are displayed by the lower and upper bounds of the box, respectively. Whisker lines depict the maximum and minimum of each climate index and in each station.

The FD elongation time (**Figure 6(a)** and **Table 1**) was the longest in the upper part of the basin, and it was the shortest in the middle. The longest annual FD period was observed in the Naryn region with an average of 163 days between 1960 and 2015 and with the longest cold days observed in 1966 (185 days) and the shortest in 2011 (139 days). The shortest duration of cold days was observed in the Karshi region where FD was 1 day

in 1997, 2004 and 2009. The longest FD period in this region was in 1984 (74 days). The lower part of the basin had a longer FD index than the middle with an average FD index of 117 days. In contrast, the SU observation period was the shortest in the upper part of the basin (**Figure 6**(**b**) and **Table 1**), meaning that the annual mean SU period was 41 days. In the middle part, i.e. in the Tashkent and Karshi regions, the longest SU period was observed with an annual maximum SU period of 177 (2012) and 214 days (2002), respectively.

The GSL duration also changed in accordance with SU, i.e. short-term GSL in the UASB, long-term in the MASB and relatively short-term GSL in the LASB (**Figure 6**(**c**) and **Table 1**). The total average GSL duration across the basin was 200 - 220 days mostly during April - October. The duration of GSL varied depending on the location, including the longest GSL duration observed in Karshi in 2009, which lasted up to 342 days. The average GSL period in this region from 1960 to 2015 was also the longest, at 301 days, compared to other regions. In the other regions, especially in Naryn and Kazalinsk, the average GSL stretch time was much shorter, i.e. 180 and 212 days, respectively. The start and end times of the GSL period varied from mid-March to the 1st half of November in the MASB, 15 days later from the 1st half of April to the end of October and from the 2nd half of April (or 1st half of May) until September in the UASB.

Karshi was the region with the longest duration of the dry process compared to other regions where the annual mean CDD period was 149 days (**Figure 6**(**d**) and **Table 1**). The mean annual CDD duration was the shortest only in Naryn (39 days), showing similar results in other regions as follows: Khatlon (87 days), Tashkent (94 days), Chimbay (86 days) and Kazalinsk (78 days). The CDD follow-up period was mainly in the summer months from June to August.

By analysing trends in all the climate indices (**Table 1**) from 1960 to 2017, we can see that the FD decreased and SU increased in selected regions. FD trend showed only a decrease in all the selected regions, and the largest FD decline was observed in Tashkent (-17 days per decade) and Kazalinsk (-13 days per decade). The largest SU increase was observed in both regions (+10 days per decade). There was also a significant increase in the SU period in the Chimbay region (+9 days per decade).

Table 1 Maximum, minimum, mean (unit: Day) and trend (unit: Days per decade) values of each climate index. FD (Frost days), SD (Summer days), GSL (Growing season length), CDD (Consecutive dry days).

Climate index		Station					
		Naryn	**Khatlon**	**Tashkent**	**Karshi**	**Chimbay**	**Kazalinsk**
FD	Max	185	150	93	71	133	159
	Min	139	97	97	97	97	97
	Mean	163	127	58	22	107	127
	Trend	-11	-9	-17	-7	-10	-13
SD	Max	69	131	177	214	177	154
	Min	10	85	138	143	124	104
	Mean	41	108	159	186	146	129
	Trend	4	6	10	7	9	10
GSL	Max	207	242	310	342	251	244
	Min	136	194	199	240	188	185
	Mean	180	221	270	301	227	212
	Trend	-9	0	12	12	9	10
CDD	Max	82	135	179	220	156	180
	Min	9	24	29	59	41	37
	Mean	39	87	94	149	86	78
	Trend	-11	-3	-2	22	10	-10

The GSL trend reversal is a negative and stable process in the upper part of the basin. The Khatlon region had no trend over the last 55 years (0 days per decade), meaning that the GSL period is stable. In the Naryn

district, the value of GSL significantly decreased (-9 days per decade) in the middle and lower parts of the basin, and the duration of GSL increased significantly, especially in Tashkent and Karshi (+12 days per decade) and in Chimbay (+9 days per decade) and Kazalinsk (+10 days per decade) where relatively low elevations were observed. An increase in the CDD trend value will lead to more incidence of the drought process in the region. The CDD trend increased only in 2 regions, i.e. Karshi (+22 days per decade) and Chimbay (+10 days per decade), while the CDD duration decreased in the other 3 regions with the largest decrease being observed in Naryn (-11 days per decade) and Kazalinsk (-10 days per decade).

Interannual change of climate variables in the ASB

Previous studies have been conducted in Central Asia to determine the time of the change of seasons [44-46]. Duration of the growing and the non-growing seasons were noted to be dependent of changes in air temperature, i.e. when mean daily air temperature was +5 ℃ and above. In terms of agriculture and plant development, the growing season is observed between March and October. It is also said that the duration of the growing season depends on the geographical location. Past studies also tried to determine the exchange process between seasons based on the precipitation and temperature changes [47].

Based on previous part, we tried to determine the inter-annual seasonal change period based on the changes in temperature and precipitation, i.e., as noted above, by analysing the 4 climate extreme index changes by dividing the region into 3 sub-regions. Summarizing the changes in climate extreme indices (FU, SU, GSL and CDD) observed in the UASB, MASB and LASB, we determined the average inter-annual seasons for the entire ASB, i.e., the growing season (April - October) and non-growing season (November - March). Based on this, we analyse the seasonal climate change below.

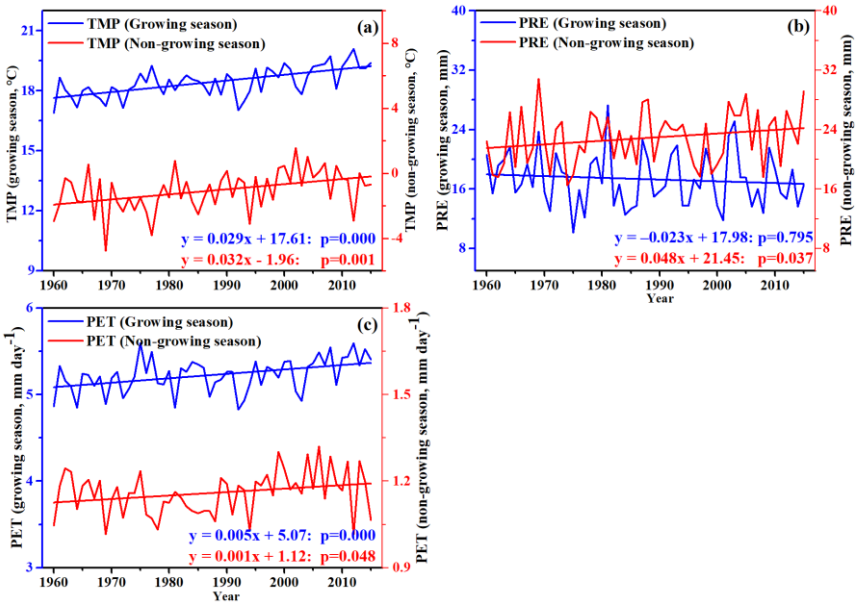

Figure 6 Long-term seasonal climate change trend over ASB between 1960 and 2017: (a) Temperature (TMP, ℃), (b) Precipitation (PRE, mm) and (c) Potential evapotranspiration (PET, mm day^{-1}). Blue line is growing season and red line is non-growing season.

The inter-annual change of temperature rate (**Figure 7**(**a**)) during the growing season was 0.29 ℃ decade^{-1}, while that during the non-growing season was 0.32 ℃ decade^{-1}. The mean values of the TMP varied from -4.8 to +1.6 ℃ and +16.9 to +20.1 ℃ during the cold and warm periods, respectively. The maximum TMP during the growing seasons recorded in 2012 was 20.1 ℃, while the minimum TMP of 16.9 ℃ was observed in the years 1960 and 1994. Similarly, for non-growing seasons, the maximum TMP value (1.6 ℃) was recorded in 2002, and the minimum TMP value (-4.8 ℃) was observed in 1969.

The cumulative mean annual precipitation in ASB in the growing season was 115 mm, and for the non-growing season it was 193 mm. As shown in the time series of mean precipitation from 1960 to 2017 (**Figure 7**(**b**)), the precipitation in the basin during the growing season showed a slowly decreasing trend over the study period, the inter-annual rate of change being -0.2 mm decade^{-1}. During the non-growing period, the precipitation trend showed a slowly rising trend over the study period with an inter-annual rate of change of 0.5 mm decade^{-1}. The maximum amount of PRE was observed in 1969 at 30.8 mm, while the deficit was observed in 1975 at 10.1 mm.

The seasonal trend of PET showed a slight increase during both seasons in the ASB (**Figure 7**(**c**)). The trend of mean PET growth was 0.051 mm day^{-1} decade^{-1} during the growing season, and the maximum PET value was noted in 2012 at 5.6 mm day^{-1} decade^{-1} and the minimum PET in 1969 around 1.01 mm day^{-1} decade^{-1} in the growing season. The annual mean of 5.23 mm day^{-1} decade^{-1} and 1.16 mm day^{-1} decade^{-1} water disappeared in the growing and non-growing seasons, respectively.

Analysis of climate change by sub-regions

Analyzing inter-annual, growing and non-growing trends over the study regions (LASB, MASB and UASB) from 1960 to 2017 (**Figure 8**), we noted that both the high value of TMP (21.9 ℃) and increase (0.31 ℃ decade^{-1}) were recorded in the LASB region (**Figure 8**(**a**)). TMP trend in the UASB region in the non-growing season demonstrates a faster increase than in the growing season (**Figure 8**(**d**)).

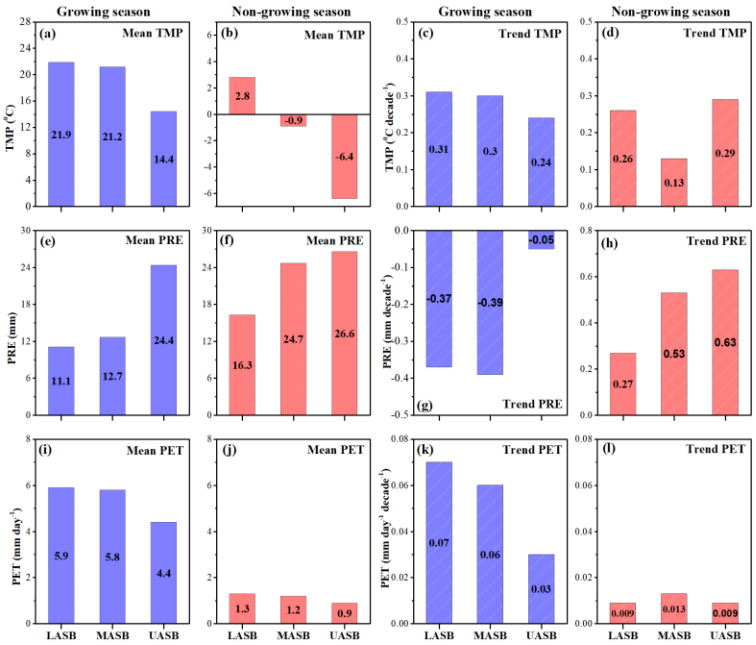

Figure 7 Trend and mean value of climatic variables in sub-regions (LASB, MASB, and UASB) in growing and non-growing periods between 1960 and 2017. (a)-(d) mean annual temperature (TMP, ℃) and its trend (℃ decade^{-1}), (e)-(h) mean annual precipitation (PRE, mm) and its trend (mm decade^{-1}) and (i)-(l) mean annual potential evapotranspiration (PET, mm day^{-1}) and its trend (mm day^{-1} decade^{-1}). The white sparse line in the box indicates the significant linear trends (90 % confidence level). The blue box presents growing season and the red box non-growing season.

Based on the regional variation of the mean PRE observation, we can assume that the 2 seasons are LASB arid and UASB wet zone (**Figures 8**(**e**) and **8**(**f**)). Seasonal PRE trend reversal was observed in the 2 seasons, i.e. only significantly negative in the growing season and significantly positive in the non-growing season. High and low mean PET values were observed in both LASB and UASB as in TMP (**Figures 8**(**i**) and **8**(**j**)). In terms

of regions, the seasonal PET trend was different from the TMP in the non-growing season, i.e. a higher PET trend was observed in the MASB, and the same trend was also observed in the other 2 regions (**Figure 8(l)**).

Conclusions

In this study, we analyse the long-term climate change observed in the ASB, and the conclusions are presented in this section. During the study period, TMP increased significantly in the basin. According to the spatial distribution of linear trends, significant increasing trends in the basin were observed above and around the Aral Sea and the south-eastern part of the basin. These trends were also positive in both growing and non-growing seasons but was higher in the non-growing season than in the growing season. In terms of the temporal TMP change during 2000 - 2017, the temperature trend was negative, while from 1960 to 2017 and 1960 to 2000, a positive trend was recorded. But, despite TMP recorded a negative trend in the last decade, in this period, the mean TMP showed a greater value compared to other periods.

The area averaged time series of mean annual PRE showed a weak increasing trend from 1960 to 2017. For the sub-time periods, the PRE decreased in the 1st period (1960 - 2000) and increased in the 2nd period (2000 - 2017). For the whole study period, the precipitation change was a process that differed diametrically over the 2 seasons during the study period with the precipitation value decreasing during the growing season and increasing during the non-growing season.

Area averaged annual PET evidenced a positive trend during the whole study period. The spatial distribution of trends of PET showed growth in the whole study area except for the northeastern part of the basin. Seasonal PET also showed positive trends in both growing and non-growing seasons.

Seasonal climate change across sub-regions indicates that LASB had higher TMP and PET, and lower PRE values during the growing season. According to the results of the analysis, LASB is a dry and hot region and UASB a humid and cold region. However, despite UASB being cold, this is the region where the temperature is increasing faster than in other sub-regions.

In this paper, we have used extreme climate index change not only to determine the period of growing and non-growing change in the region but also to explain in detail the extreme climate change in the period after the Aral Sea tragedy.

The results presented in this study can be used in the development of policies to adapt to recent climate conditions and to characterize climate vulnerability in the ASB region.

Acknowledgements

We are grateful to the Nukus branch of Tashkent University of Information Technologies named after Muhammad Al-Khwarizmi, Uzbekistan, for providing the opportunity to work on this study.

References

[1] I Haag, PD Jones and C Samimi. Central Asia's changing climate: How temperature and precipitation have changed across time, space, and altitude. *Climate* 2019; **7**, 123.
[2] F Giorgi. Climate change hot-spots. *Geophys. Res. Lett.* 2006; **33**, 01029.
[3] KMD Beurs, GM Henebry, BC Owsley and IN Sokolik. Large scale climate oscillation impacts on temperature, precipitation and land surface phenology in Central Asia. *Environ. Res. Lett.* 2018; **13**, 065018.
[4] M Zhang, Y Chen, Y Shen and B Li. Tracking climate change in Central Asia through temperature and precipitation extremes. *J. Geogr. Sci.* 2019; **29**, 3-28.
[5] Z Hu, C Zhang, Q Hu and H Tian. Temperature changes in Central Asia from 1979 to 2011 based on multiple datasets. *J. Climate* 2014; **27**, 1143-67.
[6] F Chen, W Huang, Jin, J Chen and J Wang. Spatiotemporal precipitation variations in the arid Central Asia in the context of global warming. *Sci. China Earth Sci.* 2011; **54**, 1812-21.
[7] C Reyer, IM Otto, S Adams, T Albrecht, F Baarsch, M Cartsburg, D Coumou, A Eden, E Ludi, R Marcus, M Mengel, B Mosello, A Robinson, CF Schleussner, O Serdeczny and J Stagl. Climate change impacts in Central Asia and their implications for development. *Reg. Environ. Change* 2017; **17**, 1639-50.
[8] T Bernauer and T Siegfried. Climate change and international water conflict in Central Asia. *J. Peace Res.* 2012; **49**, 227-39.

[9] S Xenarios, A Gafurov, D Schmidt-Vogt, J Sehring, S Manandhar, C Hergarten, J Shigaeva and M Foggin. Climate change and adaptation of mountain societies in Central Asia: Uncertainties, knowledge gaps, and data constraints. *Reg. Environ. Change* 2019; **19**, 1339-52.
[10] MR Bhutiyani, VS Kale and NJ Pawar. Climate change and the precipitation variations in the Northwestern Himalaya: 1866 - 2006. *Int. J. Climatol.* 2010; **30**, 535-48.
[11] T Bolch. Climate change and glacier retreat in northern Tien Shan (Kazakhstan/Kyrgyzstan) using remote sensing data. *Glob. Planet. Change* 2007; **56**, 1-12.
[12] KS Gafforov, A Bao, S Rakhimov, T Liu, F Abdullaev, L Jiang, K Durdiev, E Duulatov, M Rakhimova and Y Mukanov. The assessment of climate change on rainfall-runoff erosivity in the Chirchik-Akhangaran Basin, Uzbekistan. *Sustainability* 2020; **12**, 3369.
[13] R Feng, H Zheng and M Gan. Spatial and temporal variations in extreme temperature in Central Asia. *Int. J. Climatol.* 2018; **38**, e388-e400.
[14] EM Aizen, V Aizena, JM Melacka, T Nakamuraband and T Ohta. Precipitation and atmospheric circulation patterns at Mid-latitudes of Asia. *Int. J. Climatol.* 2001; **21**, 535-56.
[15] S Nietullaeva, B Fayzullaev, A Karimova and N Shaudenbayev. An investigation into the hydro-climate processes impacting Aral Sea Region in Central Asia. *Ann. Romanian Soc. Cell Biol.* 2021; **25**, 11692-703.
[16] J Yao and Y Chen. Trend analysis of temperature and precipitation in the Syr Darya Basin in Central Asia. *Theor. Appl. Climatol.* 2015; **120**, 521-31.
[17] T Berdimbetov, S Ilyas, Z Ma, M Bilal and S Nietullaeva. Climatic change and human activities link to vegetation dynamics in the Aral Sea Basin using NDVI. *Earth Syst. Environ.* 2021; **5**, 303-18.
[18] I Harris, PD Jones, TJ Osborn and DH Lister. Updated high-resolution grids of monthly climatic observations - the CRU TS3.10 Dataset. *Int. J. Climatol.* 2014; **34**, 623-42.
[19] U Schneider, A Becker, P Finger, A Meyer-Christoffer, M Ziese and B Rudolf. GPCC's new land surface precipitation climatology based on quality-controlled in situ data and its role in quantifying the global water cycle. *Theor. Appl. Climatol.* 2013; **115**, 15-40.
[20] J Simpson, C Kummerow, WK Tao and RF Adler. On the tropical rainfall measuring mission (TRMM). *Meteorol. Atmos. Phys.* 1996; **60**, 19-36.
[21] Z Hu, Q Li, X Chen, Z Teng, C Chen, G Yin and Y Zhang. Climate changes in temperature and precipitation extremes in an alpine grassland of Central Asia. *Theor. Appl. Climatol.* 2015; **126**, 519-31.
[22] M Xu, S Kang, H Wu and X Yuan. Detection of spatio-temporal variability of air temperature and precipitation based on long-term meteorological station observations over Tianshan Mountains, Central Asia. *Atmos. Res.* 2018; **203**, 141-63.
[23] T Berdimbetov, ZG Ma, S Shelton, S Ilyas and S Nietullaeva. Identifying land degradation and its driving factors in the Aral Sea Basin from 1982 to 2015. *Front. Earth Sci.* 2021; **9**, 690000.
[24] TT Berdimbetov, ZG Ma, C Liang and S Ilyas. Impact of climate factors and human activities on water resources in the Aral Sea Basin. *Hydrology* 2020; **7**, 30.
[25] TT Berdimbetov, Z Ma, S Nietullaeva and A Yegizbayeva. Analysis of impact of Aral Sea catastrophe on anomaly climate variables and hydrological processes. *Int. J. Geoinformat.* 2021; **17**, 65-74.
[26] ML Felix, YK Kim, M Choi, JC Kim, XK Do, TH Nguyen and K Jung. Detailed trend analysis of extreme climate indices in the upper geum river basin. *Water* 2021; **13**, 3171.
[27] TD Mitchell and PD Jones. An improved method of constructing a database of monthly climate observations and associated high-resolution grids. *Int. J. Climatol.* 2005; **25**, 693-712.
[28] A Yegizbayeva, S Ilyas and T Berdimbetov. Drought characterisation of Syrdarya River Basin in Central Asia using reconnaissance drought index. *In*: Proceedings of the IEEE International Geoscience and Remote Sensing Symposium, Kuala Lumpur, Malaysia. 2022, p. 6356-9.
[29] Y Chen, W Li, H Deng, G Fang and Z Li. Changes in Central Asia's water tower: Past, present and future. *Sci. Rep*. 2016; **6**, 35458.
[30] H Guo, A Bao, T Liu, G Jiapaer, F Ndayisaba, L Jiang, A Kurban and PD Maeyer. Spatial and temporal characteristics of droughts in Central Asia during 1966 - 2015. *Sci. Total Environ.* 2019; **628**, 1523-38.
[31] J Sillmann, VV Kharin, X Zhang, FW Zwiers and D Bronaugh. Climate extremes indices in the CMIP5 multi-model ensemble. Part 1: Model evaluation in the present climate. *J. Geophys. Res*. 2013; **118**, 1716-33.

[32] J Sillmann, VV Kharin, FW Zwiers, X Zhang and D Bronaugh. Climate extremes indices in the CMIP5 multi-model ensemble. Part 2: Future projections. *J. Geophys. Res*. 2013; **118**, 2473-93.
[33] E Duulatov, X Chen, AC Amanambu, FU Ochege, R Orozbaev, G Issanova and G Omurakunova. Projected rainfall erosivity over Central Asia based on CMIP5 climate models. *Water* 2019; **11**, 897.
[34] HJ Xu, XP Wang and XX Zhang. Decreased vegetation growth in response to summer drought in Central Asia from 2000 to 2012. *Int. J. Appl. Earth Obs. Geoinf.* 2016; **52**, 390-402.
[35] TC Peterson. Climate change indices. *WMO Bull.* 2005; **54**, 83-6.
[36] RK Jaiswal, AK Lohani and HL Tiwari. Statistical analysis for change detection and trend assessment in climatological parameters. *Environ. Process.* 2015; **2**, 729-49.
[37] JB Wijngaard, AMGK Tank and GP Können. Homogeneity of 20th century European daily temperature and precipitation series. *Int. J. Climatol.* 2003; **23**, 679-92.
[38] AN Pettitt. A non-parametric approach to the change-point problem. *J. R. Stat. Soc*. *Ser*. *C* 1979; **28**, 126-35.
[39] L Jiang, A Bao, G Jiapaer, H Guo, G Zheng, K Gafforov, A Kurban and PD Maeyer. Monitoring land sensitivity to desertification in Central Asia: Convergence or divergence? *Sci. Total Environ.* 2019; **658**, 669-83.
[40] DR Easterling, GA Meehl, C Parmesan, SA Changnon, TR Karl and LO Mearns. Climate extremes: Observations, modeling, and impacts. *Science* 2000; **289**, 2068-74.
[41] P Groisman and EY Rankova. Precipitation trends over the Russian permafrost-free zone: Removing the artifacts of preprocessing. *Int. J. Climatol.* 2001; **21**, 657-78.
[42] GA Meehl, JM Arblaster and DM Lawrence. Monsoon regimes in the CCSM3. *J. Climate* 2006; **19**, 2482-95.
[43] TR Karl, NN and A Ghazi. CLIVAR/GCOS/WMO workshop on indices and indicators for climate extremes: Workshop summary. *Clim. Change* 1999; **42**, 4.
[44] R Bohovic, P Dobrovolny and D Klein. The spatial and temporal dynamics of remotely-sensed vegetation phenology in Central Asia in the 1982 - 2011 period. *Eur. J. Remote Sens.* 2016; **49**, 279-99.
[45] N Ibragimov, SR Evett, Y Esanbekov, BS Kamilov, L Mirzaev and JPA Lamers. Water use efficiency of irrigated cotton in Uzbekistan under drip and furrow irrigation. *Agr. Water Manag.* 2007; **90**, 112-20.
[46] E Lioubimtseva. Environmental changes in arid Central Asia inferred from remote sensing data and ground observations. *Arid Ecosyst*. 2005; **11**, 67-72.
[47] G Ayzel and A Izhitskiy. Climate change impact assessment on freshwater inflow into the Small Aral Sea. *Water* 2019; **11**, 2377.